Visualization and Quantification of the Water Distribution Inside an Operating Fuel Cell by Neutron Radiography

J. Zhang[1], R. Shimoi[1], K. Shinohara[1]
D. Kramer[2], E. Lehmann[2], G. G. Scherer[2]

[1] Nissan Motor Co., Ltd., 237-8523, Japan
[2] Paul Scherrer Institut, CH-5232 Villigen, Switzerland
[*]E-mail: j-zhang@mail.nissan.co.jp

The performance of a Polymer Electrolyte Fuel Cell (PEFC) working on pure hydrogen and air is primarily limited by the performance of the cathode side. At high current density, the transport of reactant (O_2) towards to catalyst layer is the limiting process. The major obstacle for a fuel cell to realize its potential limiting current density is most probably the reduction of effective porosity due to the accumulation of liquid product water inside the flow channel, the gas diffusion layer (GDL), or the catalyst layer. An operating fuel cell was tested in the neutron radiography facility at Paul Scherrer Institut, Switzerland, to obtain neutron transmission images. The distribution of water inside a fuel cell was successfully visualized. The total amount of water in the neutron beam passage was estimated using the mass attenuation coefficient calibrated with a water wedge of known profile. Major factors influencing the presence and distribution of water were examined. The sequence of events during the flooding development is discussed in the paper.

1. Introduction

The performance of a Polymer Electrolyte Fuel Cell (PEFC) working on pure hydrogen and air is primarily limited by the performance of cathode. At low current density, the sluggish kinetics of the oxygen reduction reaction (ORR) is the limiting process, and efforts are being vigorously taken either to find a better catalyst or to increase the electrochemical area by optimizing the interface structure among catalyst and ionomer, including the porosity inside the catalyst layer.

At higher current density, the transport of reactant (O_2) becomes the limiting process, however. While the activation over-potential increases with the logarithm of current density, according to Tafel's law, the concentration overpotential increases more than exponentially near the limiting current density.

An estimation of the limiting ORR current density for a cell working on air, using the properties of the state-of-art gas diffusion layer (GDL) and assuming the absence of liquid water inside the GDL, would give a number well above 5 A/cm^2. However, most of the PEFCs can hardly operate on a current density above 2 A/cm^2 at relatively high humidification. The cell voltage, and hence the power, drops off drastically when the current density approaches its limiting value. For the applications that favor the operation near the maximum power, for example to increase the power density of the fuel cell system in a car, the elevation of the limiting current density will mean less number of cells or total active area for the same amount of power requirement and will in turn translate to the reduction of catalyst loading per unit power.

The major obstacle that prevents a fuel cell from realizing its theoretical limiting current density is most probably the diminishing of effective porosity due to the accumulation of liquid product water inside the flow channels, the GDL, or the catalyst layer. Therefore, the knowledge about the amount of liquid water inside full cell is of great technical significance.

Direct observation through a transparent plate could only give information about water inside the flow channels and at the surface (back side) of the GDL. The different surface properties of a transparent plate compared to the ones of a carbon plate also cast doubt on the generality of the observation. Therefore, it is highly desirable to have an effective means that could quantify the

liquid water distribution inside an operating fuel cell utilizing a true bipolar plate materials.

Neutron radiography is a powerful tool to visualize the interior of bodies containing materials with hydrogen as constituent, and it has been employed to investigate the water distribution inside a fuel cell, either across the membrane thickness [1] or across the membrane plane [2, 3].

Hydrogen atoms have a very low attenuation coefficient for X-rays (0.02 cm-1 at 120 kV). In contrast, the attenuation coefficient of hydrogen atoms for a neutron beam is exceptionally high (3.44 cm^{-1} for thermal neutrons). Further, the attenuation coefficient is much higher than the one of materials commonly used in the fabrication of a polymer electrolyte fuel cell, such as carbon or copper. Therefore, neutron radiography could be used as a powerful tool for the visualization of water in an operating fuel cell.

Images taken of a fuel cell after it has been purged by dry N2 gas can be used as reference images for the same cell under operation, to extract the attenuation due to the increase of the electrochemically generated water, as well as to correct for the uneven profile of the incoming neutron beam.

The mass attenuation coefficient of water has to be calibrated for these measurements, rather than taking tabulated values. This is because the available neutron beam exhibits an energy distribution, in contrast to monochromatic beams used to determine the tabulated attenuation coefficients. Furthermore, the energy-dependent detector response has to be taken into account. Calibration with a water wedge showed that the attenuation coefficient of water depends on the thickness of the water layer, due to multiple neutron scattering in thicker water layers (the discrepancy can reach up to 30% at about 1mm of water layer)

2. Experimental Methods

2.1. Visualization and Quantification Principle

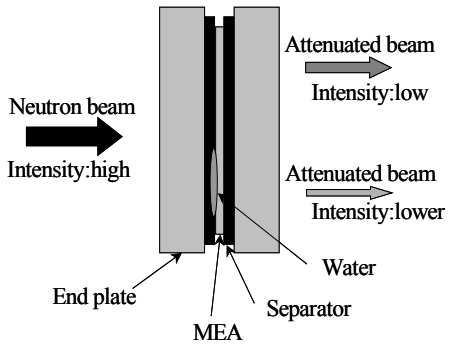

Fig. 1. Visualization principle.

The collimated neutron beam attenuates while passing through the fuel cell (Fig. 1.). The degree of attenuation depends on the amount and the attenuation coefficients of the materials in the beam pathway. The transmitted neutron beam hits the scintillator and evokes the emission of light. The light is taken up by a CCD camera and the resulting optical images are recorded by a computer.

The attenuation of the neutron beam follows the exponential law in first order. To obtain quantitative information about the amount of water inside the fuel cell, one needs to take a reference image and a signal image. A reference image is taken after the cell is purged with dry N_2 gas:

$$I_{ref} = I_0 \exp(-\Sigma_{ref} \cdot d_{ref}) \quad (1)$$

A signal image is taken while the cell is under operation:

$$I_{signal} = I_0 \exp(-\Sigma_{ref} \cdot d_{ref} - \Sigma_w \cdot d_w) \quad (2)$$

The total amount (thickness) of water in the neutron pathway could be determined by dividing the signal image with the reference image:

$$d_w = -\frac{1}{\Sigma_w} \ln\left(\frac{I_{signal}}{I_{ref}}\right) \quad (3)$$

The visualization tests were conducted in the neutron radiography facility, NEUTRA, at Paul Scherrer Institut, Switzerland [4, 5]. The CCD camera has a chip size of 1024 by 1024 pixels. The spatial resolution of the cell active area is about 0.11 mm by 0.11 mm. An exposure time of 10 s and readout time of 2 s was found to give the lowest noise in the image data.

2.2. Fuel Cell Design The tested cell had an active area of 10 by 10 cm^2. A 10-channel, 5-pass serpentine flow field, in co-flow configuration, was used to feed in and out reactant gases on both anode and cathode side. Gold plated aluminum plates were used as the current collectors and end plates.

Thin plates for the separator, current collector, and end plate are preferable to enhance the attenuation signal of water. However, on the other hand, plates with an adequate thickness are needed to ensure a uniform compaction pressure onto the separator and membrane electrode assembly (MEA), as well as a uniform temperature distribution on

both sides of the MEA. One compromise design is an aluminum plate, which is thin within the active area, to reduce the attenuation, but thick in the periphery to enhance the mechanical strength.

2.3. Operation Conditions and Test Procedure

The cell operates at 80 ī and ambient pressure. Humidified pure H_2 and air were supplied to the cell. A catalyst-coated-membrane and paper-type GDLs were used.

According to the test schedule, the specified gas cylinders are connected to the cell. The anode and cathode flow fields are supplied with the respective gases at the specified flow rates. The humidifiers are set to the specified temperatures. The current is drawn from the cell. When the system is stabilized, a neutron radiogram is taken. Prior to the test, a number of images without the fuel cell in the beam path (open beam image) are taken. Images for cell purged with dry N_2 are taken for the referencing in post-processing the data.

3. Results and Discussion

3.1. Upstream Movement of Water Front

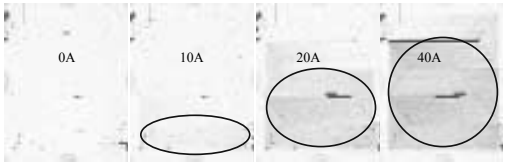

Fig. 2. Water accumulation with current.

In Fig. 2, the post-processed images at four currents are shown. The different gray levels correspond to different amounts of water. The darker the gray level of the pixel, the more water is present. In this case, both anode and cathode side were fully humidified. The stoichiometric ratios (SR) were 1.5 and 2.5 for anode side and cathode side, respectively. It is clearly visible that water starts to accumulate at the downstream of the flow field near the outlet. As more current is drawn from the cell, the portion of the active area having water accumulated extends upstream.

To get quantitative information, the whole flow field was divided into 25 segments from the inlet to the outlet, following the flow direction (Fig. 3.).
The total amount of water within each segment is integrated and plotted against the segment number, as shown in Fig. 4. Near the inlet, the change in accumulated water is small. There is more or less constant water content near the outlet. These values increase with current. Between segments at the inlet and segment at the outlet, there is a transition region, which extends itself upstream with current. Flooding seemed to occur when the water content in the downstream region reaches its maximum and the transition region cannot extend itself further upstream.

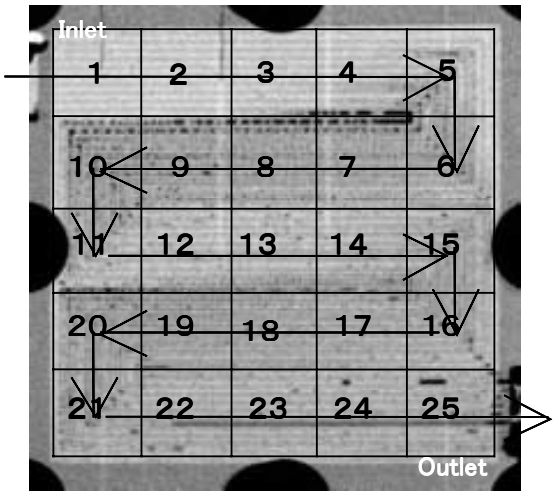

Fig. 3. Active area divided into 25 segments.

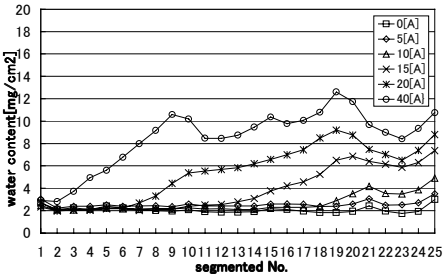

Fig. 4. Movement of water front towards upstream.

3.2. Effects of Dew Point

To investigate the effect of the dew point of inlet gases on the water distribution behavior of an operating fuel cell, the dew point of the two supplied gases was set to 55, 65 and 75 ī , respectively, and visualization was performed. The stoichiometric ratios (SR) are 1.5 and 2.5 for anode side and cathode side, respectively. At a dew point of 55 ī , essentially no water was visible. All of the product water was evaporated and being taken away by the exhaust gases. At a dew point of 65 ī , some amount of water was observed at a current value of 40 A. At a dew point of 75 ī , where the inlet gases are nearly fully humidified, the

evaporating capacity of the gas flow was greatly reduced and a substantial amount of water was observed even at a current value of 20 A.

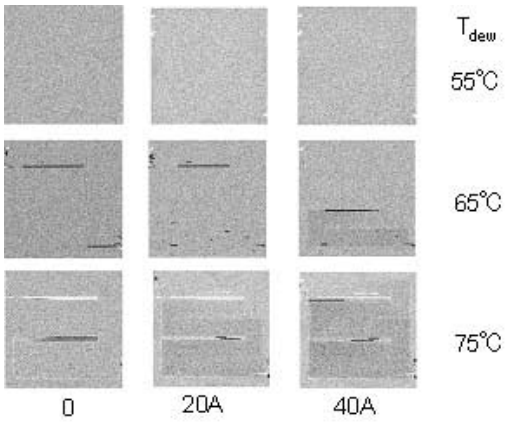

Fig. 5. Effects of dew point of inlet gases.

The dew points of both anode and cathode gases were set to 65 ī . The stoichiometric ratio of the anode gas was set to 1.5 while that of the cathode varied between 1.5 and 2.5. For higher SR (2.5), the gas flow velocity was higher, therefore most of the product water was taken away in gaseous form. In contrast, the gas flow velocity at lower SR (1.5) is slow, and its evaporating capacity is reduced and the product water can not be fully taken away by evaporation. Product water removal in liquid form (two-phase flow) is needed to maintain the water balance.

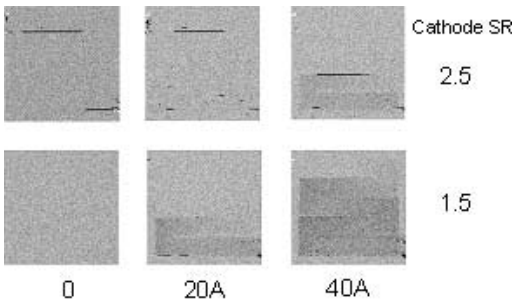

Fig. 6. Effects of stoichiometry ratio.

4. Conclusions

The distribution of water inside a fuel cell was successfully visualized. Using the mass attenuation coefficient calibrated from a water wedge, the amount of water accumulated in the path of the neutron beam was quantified.

At high current, when diffusion of O_2 becomes the limiting process, cell performance strongly depends on the water content, while at low current density, where activation processes dominate, cell performance is insensitive to water content.

Clogging of some part of the flow channels by liquid water did not necessarily cause an immediate drastic drop in cell voltage. Water inside the GDL or catalyst layer seems to be more critical for the reactant gas diffusion losses.

Both the dew points of the inlet gases and the cathode stoichiometric ratio were found to have a strong impact on the water accumulation inside a cell. High dew point and low SR tend to leave back more water inside the cell.

The flooding development in an operating cell, where the mass transport losses first increase gradually at low current density and then increase drastically at high current density, was found to be a 2- or 3-dimensional rather than a 1-dimensional phenomenon. It is suspected that flooding occurs in the following sequence: Most of water resides in the downstream region at the cathode side. The amount of water increases as the current increases. When the diffusion losses in the downstream region become dominant, more current will be generated at the upstream area. Hence, the waterfront extends itself upstream. Abrupt performance deterioration occurs when the waterfront reaches the inlet region.

Further work is needed to differentiate between the local water content in the thickness direction of the membrane-electrode-assembly.

Acknowledgements

The efforts of Mr. Stefan Hartmann, PSI, in calibrating the attenuation coefficient of water with respect to the neutron beam, are greatly appreciated.

References and Notes

[1]R. J. Bellows, M.Y. Lin, M. Arif, A.K. Thompson, and D. Jacobson, *J. of Electrochem. Soc.*, **146**(3) 1099-1103, (1999).

[2]A.B. Geiger, E. Lehmann, P. Vontobel, G.G. Scherer, A. Wokaun, Proc. *1st European PEFC Forum*, Eds. F.N. Büchi, G.G: Scherer, A. Wokaun, Lucerne, Switzerland, 2-6 July, 2001, ISBN 3-905592-08-8, p. 349-354

[3]Geiger, A.B., et al., *Fuel Cells*, **2**(2): p. 92-98. (2002).

[4]Kramer, D., et al., *Proc. 2nd European PEFC Forum*, Lucerne, ISBN: 3-905592-13-4, p. 565-574. (2003).

[5] http://neutra.web.psi.ch

[6]E. Lehmann, P. Vontobel, L. Wiezel, *Nondestr. Test. Eval.*, Vol. 16, p. 191-202 (2001)